Evaluation of a pilot-scale sewage biogas powered 2.8 kW_e Solid Oxide Fuel Cell: assessment of heat-to-power ratio and influence of oxygen content

N. de Arespacochaga[1], C. Valderrama[2], C. Peregrina[3], C.Mesa[1], L. Bouchy[4], J.L. Cortina[1]

[1] Water Technology Center CETaqua, Barcelona, Spain

[2] Department of Chemical Engineering, Universitat Politècnica de Catalunya-Barcelona Tech (UPC), Barcelona, Spain

[3] CIRSEE, Suez Environnement, France

[4] Aqualogy UK, Bristol, United Kingdom

*Correspondence should be addressed to: Nicolás de Arespacochaga

Water Technology Center CETaqua

Carretera d'Esplugues 75, 08940, Cornellà de Llobregat, Barcelona, Spain

Tel.: 93 312 48 04, Fax.: 93 312 48 00

Email: narespacochaga@cetaqua.com

Abstract

Biogas from anaerobic digestion of organic matter is a promising renewable energy source and fuel cells appear as a breakthrough technology to improve the performance of the biogas-to-energy valorisation chain. The vast majority of studies addressing biogas energy recovery through Solid Oxide Fuel Cells published in recent years correspond to simulations and lab-scale performance with synthetic biogas. This paper assesses the pilot performance of a 2.8 kW_e SOFC unit powered with cleaned sewage biogas for around 700 hours in a Wastewater Treatment Plant.

The biogas thorough treatment consisting of a biological desulphurisation with a biotrickling filter followed by a deep cleaning step based on adsorption is successful for removing sulphur

compounds, siloxanes and hydrocarbons. The influence of the heat-to-power ratio on fuel cell performance is investigated operating the system at O/C ratio of 2, reforming temperature of 550ºC, stack temperature of 800ºC and at a constant voltage of 43 V. At optimized conditions for electrical production satisfying heat demand in the WWTP, system electrical and thermal efficiencies account for 34% and 28%. Cogeneration efficiency remains constant at around 59 – 62% for all the heat-to-power ratios tested. Furthermore, the impact of the oxygen content in the biogas is also studied.

Keywords: biogas; Solid Oxide Fuel Cell; gas reforming; biogas treatment; heat-to-power ratio; energy valorisation

1. Introduction

Concerns on climate change and the end of the period of "cheap oil" prompted a broad discussion on technical and financial resources to promote increased energy efficiency in the use of resources to renewable energy. This concern has been addressed at The European Strategic Energy Technology Plan (SET) that sets a new agenda for research in the field of energy to meet the target reduction of Green House Gas (GHG) emissions by 2020 [1].

Biogas from the anaerobic digestion of organic matter is a promising energy source for its renewable nature. For example, the European primary biogas production in 2013 was 13.4 Mtoe; 21% from landfill, 9.4% from sewage and 52% from other biogas sources, such as agriculture [2]. This deposit is expected to increase around 50% by 2020. At the same time, the methane in the biogas has a global warming potential equivalent to 21 times that of CO_2; hence its conversion into renewable energy has a double environmental benefit.

However, when the biogas is used as an energy carrier for stationary application the co-generation power yields are low. Thus, in 2013 the EU produced only 52.3 TWh_e from biogas

converted mainly in internal combustion engines where the majority of the potential energy (i.e.: ~ 66%) is converted into heat [2]. In the case of energetic valorisation of biogas from wastewater treatment plants (WWTP) and landfills, this heat is usually in excess of the needs there. In addition, because of the location of these facilities, the transport of this heat to other sites is economically compromised. The result is a huge loss of heat (~ 40% of biogas in Europe) which causes poor yields of total energy. Therefore, the implementation of biogas flare without energy use is still common use.

Using biogas in a more power-efficient decentralized way requires technological breakthroughs allowing for greater power generation at the expense of low amounts of recoverable thermal energy. This alternative can be provided by fuel cells, as suggested by the roadmap of the Fuel Cells and Hydrogen Joint Technology Initiative (FCH JTI) [3]. Specifically, high-temperature fuel cells, such as Molten Carbonate Fuel Cells (MCFC) and Solid Oxide Fuel Cells (SOFC), appear to be the most suitable for the application of biogas due to their higher fuel flexibility, accepting not only hydrogen but also other fuels as syngas, natural gas and biogas [4]. Furthermore, differently from low-temperature fuel cells, such as Proton Exchange Membrane Fuel Cells (PEMFC) and Phosphoric Acid Fuel Cells (PAFC), carbon monoxide is not a poison for these systems [5], but, on the contrary, it can be used as a fuel; hence its removal is not necessary. Finally, biogas reforming in high-temperature fuel cells can be carried out within the fuel cell system (and not externally); which improves the overall energy balance [6].

However, significant problems for the operation of biogas-powered fuel cells systems are biogas contaminants. Dayton et al [5] proposed the fuel cells tolerances summarized in Table 1. Papadias et al [7] performed a detailed analysis of impurities contained in digester and landfill gas combined with a sensitivity analysis of electricity cost of a fuel cell system focusing on establishing a fitting gas-cleaning unit.

Table 1.

A series of demonstration projects have been conducted in the recent years in the USA, Japan and Europe (particularly in Germany) to demonstrate the technical feasibility of fuel cells powered with biogas. Indeed, several references of MCFC are collected by Trogisch et al [14]. Another example is the King County Carbonate Fuel Cell Demonstration Project [15], which in 2004 – 2005 coupled biogas production in a WWTP with a 1 MW_e MCFC from Fuel Cell Energy. Two relevant examples are the 1.4 MW_e MCFC unit installed in 2012 at a WWTP in California [16] and the planned 0.2 MW_e MCFC at Wyoming WWTP [17, 18]. However, technical limitations of MCFC and PAFC as a result of the use of liquid electrolytes and their high investment costs (6000 – 14000 €/$kW_{e;}$ compared to 800 – 1000 €/kW_e of internal combustion engines) have made their industrial application still very limited [19].

Today, SOFC appear to be a suitable for the application of biogas [20] as a result of the significant potential for reducing the investment cost through the development of new ceramic materials [18, 21]. The first pilot plant (1.5 kW_e) producing electricity and heat supplied by a SOFC biogas from the anaerobic fermentation of agricultural residues was operated in Germany before 2000. Other demonstrations were launched in Europe in the last decade to validate the concept. In 2001, farm biogas at Chabloz (Switzerland) powered a 1 kW_e Sulzer Hexis SOFC (Konstanz, Germany) for more than 5000 hours [22]. In 2008, Accumentrics (Westwood, USA) installed two 5 kW_e SOFCs on the scope of the BIOSOFC project (LIFE06 ENV/E/000054); one in a landfill site in Barcelona (Spain) and the other at the environmental information centre GlashusEtt in Stockholm (Sweden). However, it was necessary not only to perform a thorough cleaning of the biogas to remove contaminants but also an upgrading up to more than 80% methane. Apart from biogas upgrading, these applications externally reformed biogas upstream the stack; leading to poor thermal energy recovery.

More recently, Trendewicz and Braun [23] simulated a biogas-SOFC system for combined heat and power (CHP) applications (from 300 kW_e to 6 MW_e). The net electrical efficiency obtained was of 52% that could be further increased by 6.5% points increasing cell voltage, and a net CHP efficiency of 87.5%. Wongchanapai et al [24] analysed a direct-biogas-SOFC with a micro gas turbine (mGT) hybrid CHP system under different operating conditions. They showed that steam, as reforming agent, is better than air steam mixture for the SOFC efficiency [25].

A number of research groups have already assessed synthetic biogas powered SOFC performance at lab scale. For example, Shiratori et al [26] operated a SOFC with direct biogas using a Ni-ScSZ cermet as the anode material at the temperature of 1000°C without external reforming of the biogas; recording over 50 hours of smooth operation. Papadam et al [27] assessed the impact of the CH_4/CO_2 ratio in biogas on electrolyte-supported SOFC performance at mW range. Guerra et al [28] studied the performance of a lab-scale tubular anode supported SOFC operated at 800ºC and dry reforming conditions obtaining electrical efficiencies between 20 – 40% at different fuel utilisation and CO_2 additions.

These experiences prove the SOFC-biogas concept but show that most efforts have been devoted to the modelling of the system performance under different conditions (especially reforming) and to laboratory scale examples using synthetic biogas samples for testing of new catalyst or reactor designs [29-32]. However, scarce examples with real biogas samples powering a SOFC system at pilot scale are reported in the literature. Therefore, the aim of this paper is to evaluate the integration of SOFC systems with sewage biogas at pilot scale in a WWTP and to perform a fuel cell assessment in terms of the electric and cogeneration efficiencies under different conditions.

2. Biogas-powered SOFC cell pilot platform description

2.1 Site validation description

The biogas-powered Solid Oxide Fuel Cell (SOFC) pilot plant was installed at Mataró WWTP. The WWTP collects wastewater from different towns and villages in the Maresme region (North-East of Barcelona, Spain). The sewage treatment capacity is 30000 m^3 day^{-1} and presents a conventional sewage line with pre-treatment, primary settling and activated sludge biological reactor. The sludge line consists of primary and secondary sludge thickening, two anaerobic digesters and digested sludge centrifugation. Dewatered sludge is recycled to agriculture. Biogas production accounts for 190 Nm^3 h^{-1}, the vast majority of which is used for district heating and cooling in public buildings (hospitals, schools, public buildings, etc.). The pilot plant treated 10 Nm^3 h^{-1}, representing around 5% footprint of the full-scale.

In order to guarantee the long-term fuel cell performance, a very reliable and robust biogas treatment system was implemented upstream the fuel cell system. H_2S was the most important biogas contaminant of Mataró WWTP; hence the design of the treatment system was specifically focused on this pollutant. A two-step process was adopted: a first stage to reduce the hydrogen sulphide content down to less than 1000 ppm_v, followed by a biogas deep cleaning step to reduce its concentration to less than 0.5 ppm_v. In fact, examples of similar cascade biogas treatment units at industrial fuel cell facilities proved to be successful in reaching the fuel cell specifications [6, 14, 19]. In particular, this plant consisted of a biotrickling filter (BTF), adsorption on iron oxides, biogas drying and adsorption on activated carbon.

2.2. Biogas treatment

2.2.1. Biotrickling filter (BTF) for main H_2S removal

The BTF unit was made with a column black polypropylene (PP); square-section of 0.093 m^2 with a packed bed height of 1.8 m (total column volume of 0.17 m^3) tightly filled with HD Q-PAC® (Lantec Products Inc., USA) with 4 x 4 mm grid openings (433 m^2 m^{-3} of surface area and 88% porosity). The column operated at high liquid phase flow rate, 800 – 1.000 L h^{-1} to avoid excess

biomass removal and to reduce clogging by elemental sulphur. Temperature was maintained at 30 °C with a thermostat to provide optimal conditions of bacterial activity. No reagent addition was necessary as the WWTP effluent used provided the recommended nutrients concentrations for adequate biomass growth. The unit was operated at acidic conditions (pH 1.5) in order to promote SOB culture growth and reduce competition with non-H_2S degrading bacteria that live at higher pHs [33, 34]. Make-up water addition was controlled by pH measurements in the recirculating liquid phase. The detailed description of the BTF can be consulted elsewhere [35].

2.2.2. Biogas deep cleaning step for trace pollutants removal using iron oxide based sorbents and activated carbon

The configuration of the biogas deep cleaning step consisted of (i) iron-based adsorbent, (ii) biogas drying with refrigeration to 5 ºC and (iii) activated carbon. Two beds of each adsorbent material were placed in series with reversing capability (lead-lag operation). The iron-based adsorbent consisted of a regenerable pelleted iron-based adsorbent (diameter 2 – 4 mm and bed density 840 kg m^{-3}). Since the upstream BTF could be very sensitive to H_2S load fluctuations and could provide not stable performance in terms of removal efficiency, the iron sponge was designed to allow conservative retention times of 25 – 35 seconds (75 kg per vessel) to achieve H_2S concentrations below 0.5 ppm_v (maximum concentration accepted by the SOFC). Each vessel had a volume of 83 L (0.4 m diameter and 0.66 m height) and was operated at linear velocities of 1.3 – 2 cm s^{-1}.

The other main biogas contaminants (linear hydrocarbons and siloxanes) were removed through physical adsorption on non-impregnated extruded activated carbon (1.4 – 4 mm size and bulk density 450 kg m^{-3}). A conservative retention time of 60 seconds was selected (90 kg per vessel). Biogas drying was achieved by refrigeration in two consecutive heat exchangers: biogas first flows through a gas-gas (G/G) heat exchanger (thermal exchange surface 0.8 m^2) and afterwards through a gas-liquid (G/L) heat exchanger (thermal exchange surface 2 m^2) with water-ethylene

glycol. As moisture is condensed, some biogas pollutants are solubilised, which increases activated carbon lifetime. The detailed description of the deep cleaning step can be consulted elsewhere [36].

2.3. Energy production by Solid Oxide Fuel Cell

After the thorough biogas treatment, around 900 – 1000 NL h^{-1} directly fuelled a fully integrated SOFC unit of 2.8 kW_e nominal power (EBZ Entwicklungs- und Vertriebsgesellschaft Brennstoffzelle mbH, Dresden, Germany) operating at 850°C (the rest of the treated biogas was re-injected in the main biogas pipe). A schematic overview of the fuel cell system installed in Mataró WWTP is depicted in Figure 1. The fuel cell unit mainly consisted of two sub-systems: the electrochemical stack (2 x 1.4 kW_e) and the thermal integration unit.

Figure 1.

On the one hand, the stack (Staxera, Dresden, Germany) converted the chemical energy within the fuel into electrical energy and consisted of 2 stacks in parallel each of 60 electrolyte-supported cells (total surface area 255.6 cm^2). Cells were made of a porous nickel-based anode, a p-semi-conductor cathode (Lithium-Strontium-Manganite) and a ceramic solid electrolyte (Yttrium-Stabilized Zirconia). The generated electricity (DC at 60A/42V) was dissipated through an electronic charge, as there was no scientific interest on actually using it (a transformer and DC/AC inverter was used).

On the other hand, the heat integration unit allowed for heating gases to the operating temperature, producing steam for the internal reforming process and burning stack's off-gases to supply the required heat. It also used the remaining waste heat on the exhaust gases to produce sanitary hot water at 50°C. It basically consisted of heat exchangers, an evaporator, a reformer

and a porous after-burner. Pieces of equipment were made of Necrofer 2.4633, a high-chromium content alloy well adapted to high temperature applications, and Microtherm® wool was used as insulation material.

Gas reforming converts biogas into H_2 and CO, which are the fuels that can be electrochemically oxidised in a SOFC anode [37]. Dry reforming seems interesting for biogas applications as it is one of its major constituents; but it gives less hydrogen yield than steam reforming and has higher energy requirements (247 versus 207 kJ mol^{-1}) [30, 37-40]; hence a combination of the two reforming phenomena was chosen. The reforming mechanism can be described through Equations 1, 2 and 3.

Steam reforming: $CH_4(g) + H_2O(g) \rightarrow 3H_2(g) + CO_2(g)$ (Eq. 1)

Dry reforming: $CH_4(g) + CO_2(g) \rightarrow 2H_2(g) + 2CO(g)$ (Eq. 2)

Water Gas Shift: $CO(g) + H_2O(g) \rightarrow H_2(g) + CO_2(g)$ (Eq. 3)

Other reactions occurring within the biogas reformer are methane cracking, Boudouard reaction and reverse gasification (Equations 4, 5 and 6) [4, 41].

Methane cracking: $CH_4(g) \rightarrow 2H_2(g) + C(s)$ (Eq. 4)

Boudouard reaction: $2CO(g) \rightarrow C(s) + CO_2(g)$ (Eq. 5)

Reverse gasification: $CO(g) + H_2(g) \rightarrow C(s) + H_2O(g)$ (Eq. 6)

3. Materials and Methods

3.1. Biogas treatment monitoring

Biogas major concentration (i.e.: CH_4, CO_2, O_2 and H_2S) was on-line revealed using the biogas AwiFLEX®/AwiECO® analyzer (Awite; Germany) equipped with an infrared sensor for CH_4 and CO_2, a paramagnetic sensor for O_2 and an electrochemical sensor for H_2S. Biogas was first dried through condensation at 5ºC with a chiller, cleaned of particles with a filter and pressure adjusted with pressure regulators. The pollutant concentration in the biogas was measured before and after the

adsorption beds. Temperature and humidity measurements were also conducted using a portable Vaisala Humicap® HM70 probe. Biogas samples were also periodically off-line analysed by sampling with one-valve polypropylene fitting one litter Tedlar bags (SKC) and then quantified using an Agilent 6890 gas chromatograph (GC) equipped with an Agilent 5975 mass spectrometer (MS). Compounds were separated with a 30 m 19091s-433 column (HP-35MS 35% Phenyl Methyl Siloxane, 0.25 mm ID, 5 μm film thickness, Agilent, USA) followed by an Electron Impact (EI) mass spectrometer operated in SCAN and SIM modes. Detailed description of the methods for GC-MS analysis can be consulted elsewhere [42].

3.2. Biogas reformer conditions

The experimental rig for the investigation of the critical oxygen-to-carbon (O/C) ratio (as defined by Equation 7) for soot production is showed in Figure 2 and consisted of an electrically-driven evaporator and a reformer unit.

$$\frac{O}{C} = \frac{2n_{CO_2} + n_{H_2O}}{n_{CO_2} + n_{CH_4}} \quad \text{(Eq. 7)}$$

where: n_i is the molar flow rate of component i entering the evaporator (mol s^{-1}).

Steam was added to a synthetic mixture of CH_4 and CO_2 in order to obtain different O/C ratios. Steam and reformer temperatures were controlled by set points. Additional tests were carried out without steam addition to study soot formation at full dry conditions. Pressure loss over the reformer unit, an indicative parameter for soot production, was monitored with a diaphragm pressure switch for differential pressure DL50 E and DL5EG-1 (Elster Kromschröder, Mainz-Kastel, Germany). Constant pressure was ensured in the experimental rig by working at a constant heating power factor at the evaporator. Reformed gas composition (CH_4, CO_2, H_2, CO) was monitored using a PerkinElmer Spectrum 100 Fourier Transformed InfraRed (FTIR) spectrometer (PerkinElmer, US) equipped with a 10 cm length gas cell equipped with KBr windows. Water content in the reformed gas was monitored with a Moisture Image Series 1 Panametrics probe (GE, US).

Figure 2.

3.3. Fuel cell performance monitoring

Air and biogas flows were monitored with thermal mass flow meters; 5WK96050-Z air mass meter (Siemens VDO, Limbach-Oberfrohna, Germany) and FTAL 020CU (Honeywell, Morristown, USA) respectively. Purge gas and cooling water flows were measured with an 865 flow meter 10F7R2114111 (Gemü, Atlanta, USA) and a LABO-RRI-010 GVQ050V10KE flow meter (Honsberg Instruments, Regenstauf, Germany) respectively.

Temperature was measured by means of thermocouples type K and type N Ø 1.5 mm (SE Sensor Electric, Siegburg, Germany) and pressure was monitored with pressure transmitters CTEM70070GN4-X and CTEM7N070GL4 (Sensortechnics, Puchheim, Germany), DS 2-420 (Kalinsky Sensor Elektronik, Erfurt, Germany) and diaphragm pressure switches for differential pressure DL50 E and DL5EG-1 (Elster Kromschröder, Mainz-Kastel, Germany).

The variable loads connected to the fuel cell were regulated by a DC electronic load (4800 W maximum power input, 160 VDC and 200 A) EA-EL 9160-200HP (Elektro-Automatik, Viersen, Germany). Current transducers MRC-S-10-50-UI-DCI (Phoenix Contact, Blomberg, Germany) were used at the output of each module.

3.4. Fuel cell key performance indicators

Performance of the SOFC unit was assessed with the following parameters:

Fuel utilisation (u_f): represents the fuel not completely consumed by electrochemical reactions in the anode channel and it is defined as the ratio of fuel consumed by anode reactions to the fuel entering anode channels; and it is expressed as Equation 8:

$$U_f = \frac{n_{CH_4;transformed}}{n_{CH_4,stack\ in}} = \frac{\frac{I}{2F}}{n_{CH_4,stack\ in}} \qquad \text{(Eq. 8)}$$

where: $n_{CH4,\ stack\ in}$ is the molar flow rate of methane entering the SOFC stack (mol s^{-1}); $n_{CH4,\ transformed}$ is the molar flow rate of methane reacted within the SOFC stack; I is the current drawn from the cell (Amperes); and F is the Faraday constant (96485 C mol^{-1}).

Stack electrical efficiency (μ_e, stack): defined as the ratio of electric energy produced to the fuel energy at the stack input; and it is determined as Equation 9:

$$\mu_{e,stack} = \frac{E}{n_{CH_4,stack\ in} \cdot LHV_{CH_4}} \cdot 100 \quad \text{(Eq. 9)}$$

where: E is the electrical power production (kW_e); and LHV is the lower heating value (kJ mol^{-1}).

System electrical efficiency (μ_e, system): defined as the ratio of electric energy produced to the fuel energy at the integrated system input; and it is defined as Equation 10:

$$\mu_{e,system} = \frac{E}{(n_{CH_4,stack\ in} + n_{CH_4,afterburner\ in}) \cdot LHV_{CH_4}} \cdot 100 \quad \text{(Eq. 10)}$$

where: $n_{CH4,\ afterburner\ in}$ is the molar flow rate of methane entering the afterburner (mol s^{-1}).

Thermal power production (H) was theoretically calculated from the thermal energy available in the exhaust gases; from the exhaust gas temperature down to 120 ºC; as defined in Equation 11:

$$\mathrm{H} = \mathrm{n_{exhaust}} \cdot \mathrm{C_{p,exhaust}} \cdot (\mathrm{T_{exhaust}} - 120) \quad \text{(Eq. 11)}$$

where: $n_{exhaust}$ is the molar flow rate of exhaust gases (mol s^{-1}); $C_{p,\ exhaust}$ is the heat capacity of exhaust gases (kJ mol^{-1} K^{-1}); and $T_{exhaust}$ is exhaust gases temperature (ºC)

System thermal efficiency (μ_t, system): defined as the ratio of thermal energy produced to the fuel energy at the integrated system input; and it is defined as Equation 12:

$$\mu_{t,system} = \frac{H}{(n_{CH_4,stack\ in} + n_{CH_4,afterburner\ in}) \cdot LHV_{CH_4}} \cdot 100 \quad \text{(Eq. 12)}$$

Heat-to-power ratio: indicates the ratio of useful thermal energy to electricity generation [24]; and it is determined as Equation 13:

$$Heat - to - power = \frac{H}{E} \quad \text{(Eq. 13)}$$

Cogeneration efficiency ($\mu_{,CHP}$) is defined as the ratio of global energy production (electrical and thermal) to the fuel energy at the integrated system input; and it is defined as Equation 14:

$$\mu_{CHP} = \frac{E+H}{(n_{CH_4,stack\ in}+n_{CH_4,afterburner\ in})\cdot LHV_{CH_4}} \cdot 100 = \mu_{e,system} + \mu_{t,system} \qquad \text{(Eq. 14)}$$

4. Results

4.1 Long term evaluation of biogas quality evolution and clean-up treatment efficiency

A two-year average raw and cleaned biogas composition (compounds were gathered into general families) is collected in Table 2. As it can be seen, raw biogas was mainly polluted with H_2S, siloxanes and linear hydrocarbons. On the other hand, the concentrations of organic sulphur compounds (mainly methyl- and ethyl-mercaptane, di-methyl-sulphide, di-methyl-di-sulphide and carbon disulphide) and aromatic hydrocarbons were low. Moreover, the concentration of halogenated hydrocarbons (data not shown) was below the limits of detection for all analysis. Finally, cleaned biogas composition shows that the thorough biogas treatment proved to be successful for deep contaminant removal as the concentration of sulphur, silicon and hydrocarbons was reduced below the corresponding detection limits. Only some aromatic hydrocarbons (BTEX) were found after the biogas deep cleaning step, with values ranging 0.3 – 0.6 mg Nm^{-3}.

Table 2.

Main biogas desulphurisation was achieved at the BTF, which was operated under variable loading rates of 170 – 209 $gH_2S\ m^{-3}_{bed}\ h^{-1}$ (average 195) as a result of the variable profile of H_2S concentration. Main performance indicators were elimination capacities of 142 – 190 $gH_2S\ m^{-3}_{bed}\ h^{-1}$ (average 169) and removal efficiencies of 72 – 94% (average 84%). Notwithstanding, a 10 – 15% biogas dilution took place as a result of air injection; hence explaining the presence of O_2 and N_2 and the reduction on the CH_4 and CO_2 contents on the cleaned biogas. The detailed operating performance of the BTF can be consulted elsewhere [35].

On the other hand, biogas deep cleaning was achieved through adsorption treatment. The H_2S removal efficiency on the iron-containing adsorbent was over 99%. Because of the variations on the H_2S quality entering the deep cleaning step, two adsorbent beds in series were required to reduce H_2S content below fuel cell requirements. The average H_2S concentration after the first bed was 10 ppm_v; and it was reduced to 0.1 ppm_v at the outlet of the second bed. Removal efficiencies at the drying stage were between 5 – 15% for siloxanes, 20 – 40% for linear hydrocarbons and 15 – 25% for aromatic hydrocarbons, which is consistent with literature [43]. Finally, activated carbon proved to be an effective adsorbent for siloxanes reducing the concentration below 1 mgSi Nm^{-3}. Neither linear hydrocarbons nor siloxanes were detected after the first adsorbent bed, leading to an overall removal efficiency of 100%. In the case of aromatic hydrocarbons, the removal efficiency was of 88% as traces of these compounds were still present after the entire treatment line. The detailed operating performance of the deep cleaning step can be consulted elsewhere [36].

Overall, the results obtained for the biogas treatment system suggest that this configuration is suitable for deep biogas desulphurisation and deep removal of trace contaminants reaching the very stringent SOFC inlet requirements.

4.2. Solid Oxide Fuel Cell

4.2.1. Biogas reforming

As summarised in Table 3, lab scale tests allowed determination of the biogas reforming conditions (temperature and O/C ratio) to avoid soot formation through methane cracking, Bouduoard reactions and reverse gasification (Equations 4, 5 and 6). As it is shown, pressure drop rises were either inexistent or insignificant for all the steam reforming processes, thus the beginning or presence of soot production could not be certainly detected at any operation point. According to these tests, the reformer could be operated at an O/C ratio of 1.3 at 550 – 600°C

without risk of soot formation. On the other hand, for the biogas dry reforming tests, higher pressure drop rises were observed suggesting carbon deposition at 600°C both at O/C 1 and 1.3. These results show that the amount of CO_2 present in biogas can just partly convert biogas into H_2 and CO; thus, to avoid soot formation, a CO_2 excess is necessary far beyond the proportions observed in biogas. According to the obtained results, to reform biogas on dry conditions in a thermodynamically safe region at 625 – 650°C, an O/C ratio of 1.3 is necessary; hence biogas should be diluted to 70 – 80% with external CO_2 (CH_4:CO_2 35%:65%); consistent with tests performed by Guerra et al [28]. However, this configuration would significantly increase the operating expenses as a result of external CO_2 consumption; therefore it was discarded.

Table 3.

The reformate gas composition (molar fractions) as a function of the reforming temperature for a CH_4/CO_2 60:40 and O/C of 2.1 is shown in Figure 3. As it can be observed, methane conversion increased at higher temperatures; hence its concentration in the reformed gas decreased. Methane conversion was higher than carbon dioxide conversion because of the Water Gas Shift reaction; which produced CO_2 as a result of the excess water [24]. At 550ºC, H_2 and CO concentration accounted for 37% and 5% respectively; reaching 44% and 9% at 600ºC.

Figure 3.

The operating conditions of the reformer were set at O/C of 2 and a reforming temperature of 550ºC. The use of a high O/C ratio (higher than other references [20, 30, 37, 44]) reduces both the electrical and thermal efficiencies [4, 38], but prevented carbon deposition guaranteeing long-term SOFC operation. Furthermore, although reforming temperatures greater than 750°C are

required to achieve full methane conversion [45], 550°C was chosen in order to reduce the overall thermal demand of this stage. Therefore, reforming occurred in two separated locations: first in the reforming reactor at 550°C (Indirect Internal Reforming, IIR) and afterwards inside the stack at 850°C (Direct Internal Reforming, DIR). Under these conditions, the reforming conversion in the reformer was of 48% and the H_2/CO ratio at the reformate gas composition was 6.4, significantly greater not only than dry reforming (H_2/CO = 1) but also than steam reforming (H_2/CO = 3) as a result of the steam excess, which further converts CO into H_2 through the Water Gas Shift reaction.

4.2.2. Fuel cell performance at different heat-to-power ratios

The SOFC unit was powered with cleaned sewage biogas from Mataró WWTP (56%CH_4, 29%CO_2, 12.5%N_2, 2.5%O_2), at the reforming operating conditions previously defined during almost 700 hours. Methane and oxygen contents kept constant during the entire experimental trial; hence the fuel cell anode was powered with 0.56 moles of CH_4, 0.29 moles of CO_2, 1.12 moles of H_2O, 0.125 moles of N_2 and 0.025 moles of O_2 ($C_{0.85}H_{4.48}O_{1.75}N_{0.25}S_0$). Several biogas heat-to-power ratios (0.5, 0.8, 1.4, 1.8 and 3.1) were assessed by changing the biogas burner/stack ratio. Voltage was set up at around 43 V (i.e.: 0.72 V per cell) for all the experiments. Figure 4 depicts the operational performance of the fuel cell during the five experimental tests performed.

Figure 4.

Test 1 was operated at a biogas burner/stack ratio around 0% in order to maximise the electrical power production. As no biogas was directly introduced into the burner, thermal self-sufficiency relied on using the remaining energy in the stack output; hence the stack had to be operated at a

low fuel utilisation of 58%. At steady state (from hour 9 to hour 80), electrical and thermal power production accounted for 2023 W_e and 1023 W_t respectively; leading to a heat-to-power ratio of 0.5. System electrical and thermal efficiencies were of 41% and 21%. However, as it can be observed, operation under these conditions was not stable; cathode outlet temperature progressively decreased from 820ºC (hour 24) to 718ºC (hour 80) and finally below 650ºC (hour 100); which forced the fuel cell to automatically shut down due to the low temperature levels. As lower fuel utilisation values in the stack were not recommended, it was concluded that the SOFC unit required some biogas feeding to the afterburner to operate in thermal self-sufficient conditions, hence heat-to-power ratios larger than 0.5 were applied.

The biogas burner/stack ratio was increased: 25% in Test 2, 50% in Test 3, 58% in Test 4 and 72% in Test 5. Under these conditions, the additional heat production allowed thermally stable operation (i.e.: no reduction on the cathode outlet temperature was observed), thus no automatic shut downs occurred again. In addition, by increasing the biogas burner/stack ratio it was possible to increase the fuel utilisation in the stack, from 58% in Test 1 to 77% in Test 5. Nevertheless, electrical power production progressively decreased on each Test (1695, 1174, 1053 and 763 W_e), consistently with the reduction on the current drawn from the cell (39, 27, 24 and 18 A) and with the increase in thermal power production (1393, 1676, 1880 and 2389 W_t). The most significant operating parameters obtained during each experimental test are collected in Table 4.

Table 4.

Figure 5 shows the SOFC efficiencies (stack electrical, system electrical, thermal and cogeneration) as a function of the heat-to-power ratio. As it is depicted, the lower the heat-to-power ratio, the higher the system electrical efficiency obtained because the fuel cell is operated

425 towards electricity generation. On the other hand, the stack electrical efficiency follows an
426 opposite profile as a result of increased fuel utilisation at high heat-to-power ratios. The positive
427 relationship between u_f (up to 70 – 75%) and stack electrical efficiency is consistent with previous
428 authors [23,28,29]. Moreover, cogeneration efficiency remained more or less constant at 59 –
429 62% for the entire heat-to-power range tested.
430
431 **Figure 5.**
432
433 Van Herle et al [46] simulated the performance of a steam-reformed biogas powered 134 kW_e
434 SOFC unit obtaining 48.66% and 39.58% system electrical and thermal efficiencies respectively;
435 significantly larger than the values obtained in this study. The simulation of a 3 kW_e SOFC unit
436 (similar to the one tested in Mataró) reported stack and system electrical efficiencies of 46.5%
437 and 41.5% respectively [40]; which are still higher to this study. Moreover, other simulation-based
438 studies also reported efficiencies on this higher range [23,47,48]. However, experimental results
439 (both lab- and pilot-scale) with SOFC technology today are far away from these limits. For
440 example, Papurello et al [49] obtained a maximum stack electrical efficiency of 34% when
441 powering a 500 W_e SOFC unit with real biogas from organic waste digestion (fuel utilisation at
442 55%); which is consistent with this work. Unfortunately, no other study assessing the efficiency of
443 SOFC units using real or synthetic biogas was identified. Within this context, it is concluded that
444 additional pilot experiences are required in the future to overcome the technology gaps between
445 simulations and experimental results and to provide with reliable technico-economic data for
446 SOFC technology deployment.
447
448 **4.2.3. Energy balance for a sewage biogas powered-SOFC**

In most WWTPs, thermal energy requirements are directly linked to sewage sludge heating for anaerobic digestion (except for sludge drying facilities). Depending on geometry of the anaerobic digester, the insulation material and ambient temperatures, mesophilic anaerobic digesters have thermal energy requirements at around 20 – 35% of the biogas production [50,51], which is usually provided by the CHP unit. Therefore, thermal power productions greater than sludge heating requirements would result in heat losses; hence the recommended operating conditions for sewage biogas-powered SOFC would correspond to those showing thermal efficiencies on that range; i.e.: Test 2/Test 3. An energy balance of Test 2 is depicted in Figure 6. The total power input of 5030 W_{th}, which corresponds to the fuel feed, is split in two streams: 75% is leaded to the reforming reactor where it is upgraded to 4061 W_{th} (increment of 7.8%) and the remaining 25% is introduced in the after-burner. On the stack side, 65% of the reformed gas energy is converted inside the stack (i.e.: fuel utilisation = 65); into electricity (1695 W_e) and into stack-generated heat (945 W, also named "stack cooling power" [46]). This generated heat is dissipated both through the endothermal reforming requirements and cathode air cooling. The remaining 35% of reformate gas energy (1 – u_f) is converted into heat, together with the biogas directly introduced, in the after-burner, in order to cope with the thermal needs of the system. After the entire heat integration, exhaust gas allows for 1393 W_t exploitable low-temperature heat recovery (down to a temperature of 120 ºC). Overall, the electric (stack and system's) and cogeneration efficiencies were of 45%, 34% and 62%.

Figure 6.

4.2.4. Effect of the oxygen content in biogas on SOFC performance

The BTF control system used oxygen content in the treated gas as control variable in order to adjust the air flow requirements to carry out desulphurisation. As a result, the oxygen

concentration in the biogas remained constant at around 2.5% during the entire experimental trial. Oxygen is a poison for the anode materials; but it does not pose a risk to fuel cell operation as it is completely converted in the biogas reformer before entering the SOFC stack through the Partial Oxidation reaction (POX; Equation 15) [20].

POX reaction: $CH_4(g) + 0.5O_2(g) \rightarrow CO(g) + 2H_2(g)$ (Eq. 15)

The effect of the oxygen concentration on SOFC performance was assessed by changing the set point of the BTF control system. The SOFC unit was operated for 24 hours at oxygen concentrations of 0, 1.5 and 3.5%; which resulted in O_2/CH_4 ratios of 0, 0.03 and 0.07 respectively. Note that higher oxygen set points resulted as well in higher nitrogen contents; hence methane concentration decreased at a higher extent than the oxygen concentration increase (66, 60 and 53%). Regardless the BTF was operated under oxygen limited conditions (at 0 and 1.5%), downstream adsorbent materials could reduce H_2S concentrations below 0.1 ppm_v; hence full desulphurisation was achieved and the SOFC unit was operated under safe conditions [35]. Tests were run at a constant cell voltage of around 43 V (0.7 V per cell). As Figure 7 shows, higher O_2/CH_4 ratios reduced the electrical efficiency due to partial biogas consumption in the reformer through the POX reaction before the stack. Electrical power production accounted for 2052, 1838 and 1536 W respectively; which is explained both by the higher selectivity of POX reforming (versus steam reforming) and by the reduction in the methane content. Moreover, thermal efficiency increases as POX contributes to autothermal biogas reforming, reducing thermal requirements in the biogas reformer and increasing the temperature in the exhaust gases.

Van Herle et al [38] simulated the effect of oxygen concentration on a biogas powered SOFC reformed through POX. A reduction in the electrical performance from 32.8 to 30.5% was observed when the O_2/CH_4 ratio increased from 0.3 to 0.6. According to the results presented in this paper, residual oxygen presence in the biogas, even when the selected reforming option is

steam/dry reforming, causes an relevant reduction in the fuel cell electrical performance; accordingly biogas treatment technologies other than BTF should be selected if maximisation of electrical power production is fostered. For example, bio-scrubbers (or other scrubbing technologies, [36]), although having higher operating costs due to NaOH consumption, can fully overcome this drawbacks and would probably a better alternative for main desulphurisation in fuel cell applications.

Figure 7.

5. Conclusions

A pilot scale 2.8 kW_e SOFC unit (two 1.4 kW_e-stack in parallel with 60 electrolyte-supported cells each) was powered with cleaned sewage biogas for around 700 hours in a Wastewater Treatment Plant in Spain. Biogas reforming conditions were set at an O/C ratio of 2 (through steam addition) and a reforming temperature of 550ºC to avoid soot formation and guarantee long-term fuel cell operation. On the other hand, the SOFC stack was operated at 800ºC and at a constant voltage of 43 V (0.7 V per cell).

At optimized conditions for electrical power production satisfying heat demand in the WWTP, system electrical and thermal efficiencies accounted for 34% and 28%; and the heat-to-power ratio was 0.8. Although stack electrical efficiencies of 52 – 53% were obtained at fuel utilisations of 75 – 77%, biogas use in the after-burner was required to achieve thermal self-sufficiency; which reduced system electrical efficiency. Moreover, cogeneration efficiency remained constant at around 59 – 62% for all the heat-to-power ratios tested. The obtained efficiency levels are lower compared to simulation-based performances, which highlights the necessity for more pilot experimentation at this scale (rather than simulations) to overcome the barriers for SOFC technology deployment in WWTP. Future works should focus on the optimization of the system

524 by improving the thermal integration of the unit and the reforming conditions to allow operation at
525 lower heat-to-power ratios and at reduced thermal demand.
526 Finally, the selected biogas treatment system combining biological desulphurisation and deep
527 cleaning through adsorption proved to be to be suitable and reliable solution for fuel cell
528 applications. However, as experiments at different oxygen levels showed, the biotrickling filter
529 caused biogas dilution, increasing the oxygen and nitrogen contents in the treated gas; which had
530 a negative effect on fuel cell electrical performance. As a result, bio-scrubbers (or other scrubbing
531 technologies not injecting oxygen in the biogas) followed by adsorption would be recommended
532 for fuel cell applications.
533

534 **Acknowledgments**

535 Authors would like to thank LIFE+ programme for the financial support to carry out this study
536 (BIOCELL project LIFE07 ENV / E / 000847, www.life-biocell.eu) and the project stakeholders
537 (Agència Catalana de l'Aigua, Entitat Metropolitana de Mediambient, Consell Comarcal del
538 Maresme, Entidad de Saneamiento de la Región de Murcia, Aquagest Medioambiente and
539 Aqualogy). The authors gratefully acknowledge Pau Serra and Eva Torrecillas from Mataró
540 WWTP; and Fernando Cabello from Consell Comarcal del Maresme, for its cooperation during
541 the experimental trials.
542

543 **References**

544 [1] T.A.B. Smit, Jing Hu, Robert Harmsen. Unravelling projected energy savings in 2020 of EU
545 Member States using decomposition analyses. Energy Policy 74 (2014) 271–285.
546 [2] Eurobserver. Biogas Barometer. November 2014. http://www.energies-
547 renouvelables.org/observ-er/stat_baro/observ/baro224_Biogas_en.pdf. (Accessed online March
548 2015).

549 [3] Fuel Cell and Hydrogen technologies in Europe. Financial and technology outlook on the
550 European sector ambition 2014- 2020. http://www.fch-
551 ju.eu/sites/default/files/111026%20FCH%20technologies%20in%20Europe%20-
552 %20Financial%20and%20technology%20outlook%202014%20-%202020_0.pdf. (Accessed
553 online March 2015).
554 [4] J. Larminie and A. Dicks, Fuel cells systems explained, second ed., John Wiley and Sons,
555 West Sussex, England 2003.
556 [5] D.C. Dayton, M. Ratcliff, R. Bain, Fuel Cell Integration – A study of the impacts of gas quality
557 and impurities, Milestone Completion Report, National Renewable Energy Laboratory, Oak
558 Ridge, U.S. 2001.
559 [6] R.J. Spiegel, J.L. Preston, Test results for fuel cell operation on anaerobic digester gas, J.
560 Power Sources 86 (2000) 283-288.
561 [7] D.D. Papadias, S. Ahmed, R. Kumar, Fuel quality issues with biogas energy - An economic
562 analysis for a stationary fuel cell system, Energy 44 (2012) 257-277.
563 [8] K. Ledjeff-Hey, J. Roes, R. Wolters, CO_2-scrubbing and methanation as purification system for
564 PEF, J. Power Sources 86 (2000) 556-561.
565 [9] Fuel Cell Handbook 5th Edition, Report prepared by EG&G Services, Parsons, Inc. and
566 Science Applications International Corporation under contract no. DE-AM26-99FT40575 for the
567 U.S. Department of Energy, National Energy Technology Laboratory, October 2000.
568 [10] K. Kordesch, G. Simader, Fuel Cells and Their Applications. VCH
569 Verlagsgesellschaft:Weinheim, Germany 1996.
570 [11] R.J. Spiegel, J.L. Preston, J.C. Trocciola, Fuel cell operation on landfill gas at Penrose
571 Power Station, Energy 24 (1999a) 723-742.
572 [12] S.J. Bossart, D.C. Cicero, C.M. Zeh, R.C. Bedick, Gas Stream Cleanup, Technical Status
573 Report, Morgantown Energy Technology Center Report No. DOE-METC-91/0273, 1990.

574 [13] K.V. Lobachyov, H.J. Richter, An advanced integrated biomass gasification and molten fuel
575 cell power system, Energy Convers. Manage. 39 (1998) 1931-1943.
576 [14] S. Trogisch, J. Hoffmann, L. Daza, Operation of molten carbonate fuel cells with different
577 biogas sources: A challenging approach for field trials, J. Power Sources 145 (2005) 632–638.
578 [15] D. Rastler, King County Carbonate Fuel Cell Demonstration Project Case Study of a 1-MW
579 Fuel Cell Power Plant Fueled by Digester Gas, 1011472 Interim Report, February 2005.
580 [16] Fuel Cell Today, Fuel Cell Converting Waste to Energy Comes Online at San Jose Facility,
581 Sept 28 2012. http://www.fuelcelltoday.com/news-events/newsarchive/2012/september/fuel-cell-
582 converting-waste-to-energy-comesonline-at-san-jos%C3%A9-facility. (Accessed online March
583 2015).
584 [17] Fuel Cell Energy News Release, Fuel Cell Energy to Deliver Carbon Neutral Stationary Fuel
585 Cell Power Plant for Data Center Project with Microsoft Corporation and State of Wyoming, Nov
586 2012. http://fcel.client.shareholder.com/releasedetail.cfm?ReleaseID=722316. (Accessed online
587 March 2015).
588 [18] N.S. Siefert, S. Litster, Exergy & economic analysis of biogas fueled solid oxide fuel cell
589 systems, J. Power Sources 272 (2014) 386-397.
590 [19] R.J. Spiegel, J.L. Preston, Technical assessment of fuel cell operation on landfill gas at the
591 Groton, CT, landfill, Energy 28 (2003) 397–409.
592 [20] J. Xuan, M.K.H. Leung, D.Y.C. Leung, M. Ni, A review of biomass-derived fuel processors for
593 fuel cell systems, Renewable Sustainable Energy Rev. 13 (2009) 1301–1313.
594 [21] R. Bove, P. Lunghi, Experimental comparison of MCFC performance using three different
595 biogas types and methane, J. Power Sources 145 (2005) 588–593.
596 [22] J. Van herle, Y. Membrez, O. Bucheli, Biogas as a fuel source for SOFC co-generators, J.
597 Power Sources 127 (2004) 300–312.

598 [23] A.A. Trendewicz, R.J. Braun, Techno-economic analysis of solid oxide fuel cell-based
599 combined heat and power systems for biogas utilization at wastewater treatment facilities, J.
600 Power Sources 233 (2013) 380-393.
601 [24] S. Wongchanapai, H. Iwai, M. Saito, H. Yoshida, Performance evaluation of a direct-biogas
602 solid oxide fuel cell-micro gas turbine (SOFC-MGT) hybrid combined heat and power (CHP)
603 system, J. Power Sources 223 (2013) 9-17.
604 [25] E. Bocci, A. Di Carlo, S.J. McPhail, K. Gallucci, P.U. Foscolo, M. Moneti, M. Villarini, M.
605 Carlini, Biomass to fuel cells state of the art: A review of the most innovative technology solutions,
606 Int. J. Hydrogen Energy 39 (2014) 21876-21895.
607 [26] Y. Shiratori, T. Oshima, K. Sasaki, Feasibility of direct-biogas SOFC, Int. J. Hydrogen Energy
608 33 (2008) 6316-6321.
609 [27] T. Papadam, G. Goula, I.V. Yentekakis, Long-term operation stability tests of intermediate
610 and high temperature Ni-based anodes' SOFCs directly fueled with simulated biogas mixtures,
611 Int. J. Hydrogen Energy 37 (2012) 16680-16685.
612 [28] C. Guerra, A. Lanzini, P. Leone, M. Santarelli, D. Beretta, Experimental study of dry
613 reforming of biogas in a tubular anode-supported solid oxide fuel cell, Int. J. Hydrogen Energy 38
614 (2013) 10559-10566.
615 [29] D. Papurello, R. Borchiellinia, P. Bareschino, V. Chiodo, S. Freni, A. Lanzini, F. Pepe, G.A.
616 Ortigoza, M. Santarelli, Performance of a Solid Oxide Fuel Cell short-stack with biogas feeding,
617 Appl. Energy 125 (2014) 254–263.
618 [30] S. Farhad, Y. Yoo, F. Hamdullahpur, Effects of fuel processing methods on industrial scale
619 biogas-fuelled solid oxide fuel cell system for operating in wastewater treatment plants, J. Power
620 Sources 195 (2010) 1446–1453.

621 [31] A. Lanzini, P. Leone, M. Pieroni, M. Santarelli, D. Beretta, S. Ginocchio, Experimental
622 Investigations and Modeling of Direct Internal Reforming of Biogases in Tubular Solid Oxide Fuel
623 Cells, Fuel Cells 11 (2011) 697–710.
624 [32] M. Ni, Modeling and parametric simulations of solid oxide fuel cells with methane carbon
625 dioxide reforming, Energy Convers. Manage. 70 (2013) 116–129.
626 [33] S. Chaiprapat, R. Mardthing, D. Kantachote, S. Karnchnawong, Removal of hydrogen
627 sulphide by complete aerobic oxidation in acidic biofiltration, Process Biochem. 46 (2011) 344–
628 352.
629 [34] B. Charnnok, T. Suksaroj, P. Boonswang, S. Chaiprapat, Oxidation of hydrogen sulfide in
630 biogas using dissolved oxygen in the extreme acidic biofiltration operation, Bioresour. Technol.
631 131 (2013) 492–499.
632 [35] N. de Arespacochaga, C. Valderrama, C. Mesa, L. Bouchy, J.L. Cortina, Biogas biological
633 desulphurisation under extremely acidic conditions for energetic valorisation in Solid Oxide Fuel
634 Cells, Chem. Eng. J. 255 (2014a) 677–685.
635 [36] N. de Arespacochaga, C. Valderrama, C. Mesa, L. Bouchy, J.L. Cortina,Biogas deep clean-
636 up based on adsorption technologies for Solid Oxide Fuel Cell applications, Chem. Eng. J. 255
637 (2014b) 593–603.
638 [37] B. Tjaden, M. Gandiglio, A. Lanzini, M. Santarelli, M. Ja□rvinen, Small-Scale Biogas-SOFC
639 Plant: Technical Analysis and Assessment of Different Fuel Reforming Options, Energy Fuels 28
640 (2014) 4216−4232.
641 [38] J. Van herle, F. Marechal, S. Leuenberger, D. Favrat, Energy balance model of a SOFC
642 cogenerator operated with biogas, J. Power Sources 118 (2003) 375–383.
643 [39] P. Piroonlerkgul, S. Assabumrungrat, N. Laosiripojana, A.A. Adesina, Selection of
644 appropriate fuel processor for biogas-fuelled SOFC system, Chem. Eng. J. 140 (2008) 341–351.

645 [40] A. Lanzini, P. Leone, Experimental investigation of direct internal reforming of biogas in solid
646 oxide fuel cells, Int. J. Hydrogen Energy 35 (2010) 2463−2476.
647 [41] K. Kendall, C.M. Finnerty, G. Saunders, J.T. Chung, Effects of dilution on methane entering
648 an SOFC anode, J. Power Sources 106 (2002) 323–327.
649 [42] J. Ellner, R. Schmersahl, V. Scholz, Determination of trace compounds in biogas, reformate
650 and evaluation of its effect on PEM fuel cell performance, Proceedings of International
651 Conference on Agricultural Engineering 2008, Hersonissos, Greece, 23-25 June, OP-415.
652 [43] M. Hagmann, E. Hesse, P. Hentschel, T. Bauer, Purification of biogas-removal of volatile
653 silicones. In: Proceedings Sardinia, Eighth international waste management and landfill
654 symposium, 2001; vol. II:641–4.
655 [44] Y. Yi, A.D. Rao, J. Brouwer, G.S. Samuelsen, Fuel flexibility study of an integrated 25 kW
656 SOFC reformer system, J. Power Sciences 144 (2005) 67-76.
657 [45] Y. Shiratori, T. Oshima, K. Sasaki, Feasability of direct biogas SOFC, Int. J. Hydrogen
658 Energy 33 (2008) 6316-6321.
659 [46] J. Van herle, F. Maréchal, S. Leuenberger, Y. Membrez, O. Bucheli, D. Favrat, Process flow
660 model of solid oxide fuel cell system supplied with sewage biogas, J. Power Sources 131 (2004)
661 127-141.
662 [47] S. Farhad, F. Hamdullahpur, Y. Yoo, Performance evaluation of different configurations of
663 biogas-fuelled SOFC micro-CHP systems for residential applications, International Journal of
664 Hydrogen Energy 35 (2010): 3758-3768
665 [48] P. Dokmaingam, S. Assaburungrat, A. Soottitantawat, N. Laosiripojana, Modelling of tubular-
666 designed solid oxide fuel cell with indirect internal reforming operation fed by different primary
667 fuels. Journal of Power Sources 195 (2010): 69-78

668 [49] D. Papurello, A. Lanzini, L. Tognana, S. Silvestri, M. Santarelli, Waste to energy: Exploitation
669 of biogas from organic waste in a 500Wel solid oxide fuel cell (SOFC) stack. Energy 85 (2015):
670 145-158.
671 [50] K.D. Monson, S.R. Esteves, A.J. Guwy, R.M. Dinsdale, Anaerobic Digestion of
672 Biodegradable Municipal Wastes: A Review. University of Glamorgan, Pontypridd, Wales, 2007.
673 [51] M. Berglund, P. Börjesson, Assessment of energy performance in the lifecycle of biogas
674 production, Biomass Bioenergy 30 (2006) 254-266.
675

Table 1. Fuel Cell Tolerances adapted from Dayton et al [5]

	PEMFC	PAFC	MCFC	SOFC
Operating temperature (°C)	70 – 90	160 – 210	600 – 700	800 – 1000
H_2	Fuel	Fuel	Fuel	Fuel
CO_2	Diluent	Diluent	Re-circulated	Diluent
CO	Poison 10 ppm_v[a,b]	Poison 10 ppm_v[b]; 1% at anode[c]	With water –shifted to make H_2	With water –shifted to make H_2
CH_4	Inert, Fuel with reformer	Inert, Fuel with reformer	Fuel –reformed internally or externally	Fuel –reformed
C_2-C_6		Poison - <0.5% olefins	Plugging & coking Fuel w/reformer Sat HC – 12% vol[e] (CH4 included) Olefins - 0.2 vol%[e] Aromatics – 0.5 vol[e]% Cyclics – 0.5 vol%[e]	Fuel – similar to MCFC in regards to high molecular weight HC's
Particulates			10 ppm_w[e]; <0.1g/l of particles > 3µm[c]	
Trace Species:	ppm, dry basis			
Sulphur		Poison < 20ppm_v H_2S[c] < 50 ppm_v H_2S + COS[c]	Poison < 10 ppm H_2S in fuel < 1 ppm SO_2 in oxidant <0.5 ppm H_2S[c] <0.1 ppm H_2S	Poison <1 ppm_v H_2S[c]
NH_3		Poison < 0.2 mole% ammonium phosphate in electrolyte[c]	Fuel?/Inert - < 1vol%[c]	Fuel < 5000 ppm_v[c]
Halogens (HCl)		Poison 4ppm_v[d]	Poison < 1 ppm_v[c] <0.1 ppm_v	Poison - <1ppm_v[c]
Alkali metals			Electrolyte loss 1-10 ppm_v[f]	
Other	Water maintenance		Electrolyte balance with CO_2 recirculation	SiO_2 deposition

[a] [8]; [b] [9]; [c] [10]; [d] [11]; [e] [12]; [f] [13]

Table 2. Raw and clean biogas composition over 12-months at 30ºC and 25 – 30 mbar(g)

Compound/trace	Family	Units	Raw Biogas	Cleaned Biogas
CH_4	**Major**	**%**	59.3 – 70.2	55.1 – 57.8
CO_2	**Major**	**%**	33.1 – 37.3	28.5 – 32.5
N_2	**Major**	**%**	0.5 – 1	7.5 – 12.5
O_2	**Major**	**%**	0.2 – 0.3	1.8 – 2.9
Relative humidity (RH)	**Major**	**%sat**	80 – 100	100
H_2S	**Inorganic Sulphur**	**ppm_v**	2100 – 4350	udl(0.1)
Methyl mercaptan	**Organic Sulphur**	**mg Nm^{-3}**	0.3 – 0.8	udl(0.1)
Ethyl mercaptan	**Organic Sulphur**	**mg Nm^{-3}**	0.1 – 0.9	udl(0.1)
Dimethyl sulphide (DMS)	**Organic Sulphur**	**mg Nm^{-3}**	0 – 0.1	udl(0.1)
Dimethyl disulphide (DMDS)	**Organic Sulphur**	**mg Nm^{-3}**	udl(0.1)	udl(0.1)
Sum Linear HC	**Alkanes**	**mg Nm^{-3}**	31.9 – 47.9	udl
Sum BTEX	**Aromatic**	**mg Nm^{-3}**	3.8 – 4.8	0.3 – 0.6
Sum org. Silicium compounds	**Organic silicon**	**mg Nm^{-3}**	13.7 – 16.7	udl(0.1)
Sum of Silicium	**Organic silicon**	**mg Nm^{-3}**	3.8 – 4.9	udl(0.1)

udl: under detection limit

Table 3. Soot formation tests for biogas-steam and biogas-dry reforming

Reforming conditions	CH_4 flow rate (NL min^{-1})	CO_2 flow rate (NL min^{-1})	Steam flow rate (g/h)	O/C	T (ºC)	Test duration (h)	Pressure drop rise (mbar)	Soot production
Steam	2.5	1.7	247	2.1	500	55	0	No
Steam	2.5	1.7	247	2.1	550	47	-0.5	No
Steam	2.5	1.7	247	2.1	600	35	-0.5	No
Steam	2.5	1.7	140	1.5	550	93	0	No
Steam	2.5	1.7	102	1.3	550	167	-0.5	No
Steam	2.5	1.7	101	1.3	575	48	0	No
Steam	2.5	1.7	102	1.3	600	241	0.5	No
Dry	2.5	2.5	0	1	600	6	1.8	Yes
Dry	1.6	3.0	0	1.3	600	17	0.8	Yes
Dry	1.6	3.0	0	1.3	625	25	0	No
Dry	1.6	3.0	0	1.3	645	56	0	No

Table 4. Experimental performance of the biogas-powered SOFC unit compared to simulation

			Unit	Experimental results				
				Test 1	Test 2	Test 3	Test 4	Test 5
Duration			hours	100	160	120	180	120
INPUTS	FUEL	Biogas-to- burner	NL min^{-1}	0.05	3.86	7.38	8.44	11.53
		Biogas-to-stack	NL min^{-1}	15.08	11.52	7.55	6.31	4.40
		Burner/Stack	%	0.4	25.1	49.4	57.2	72.4
		CH_4 content	%	55.9	56.1	55.3	55.3	56.2
		CO_2 content	%	29.9	29.5	29.4	30.3	29.6
		O_2 content	%	2.42	2.49	2.58	2.62	2.50
OUTPUTS	ELECTRICAL	Current	A	47.4	39.4	26.7	23.9	17.8
		Voltage	V	42.7	43.1	43.9	44.0	42.9
		Fuel Utilisation	%	57.8	65.0	69.4	75.3	76.7
		Electrical Power	W	2023	1695	1174	1053	763
		Stack electrical efficiency	%	41.4	45.0	48.3	52.3	53.1
		System electrical efficiency	%	41.2	33.7	24.4	22.1	14.7
		Stack temperature (cathode out)	ºC	775	796	802	804	805
		Thermal self-sufficiency	-	No	Yes	Yes	Yes	Yes
	THERMAL	Exhaust gas temperature	ºC	148	163	178	191	212
		Thermal Power	W	1023	1393	1676	1880	2389
		Thermal efficiency	%	20.8	27.7	34.9	39.7	45.9
	CHP	Heat-to-power ratio	-	0.50	0.82	1.42	1.79	3.13
		Cogeneration efficiency	%	62.0	61.5	59.3	61.9	60.1

Figure 1 in word format

Click here to download Figure(s): Figure 1 in word format.docx

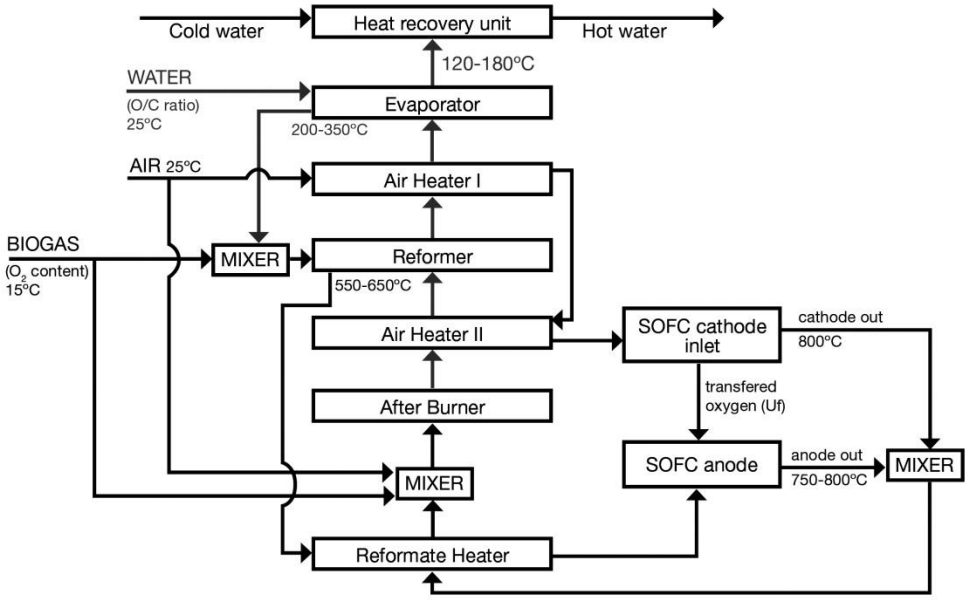

Figure 1

Figure 2 in word format

Click here to download Figure(s): Figure 2 in word format.docx

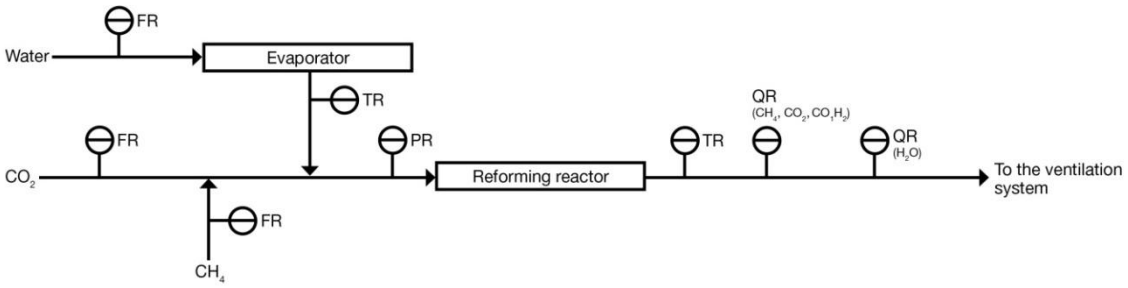

Figure 2

Figure 3 in word format
Click here to download Figure(s): Figure 3 in word format.docx

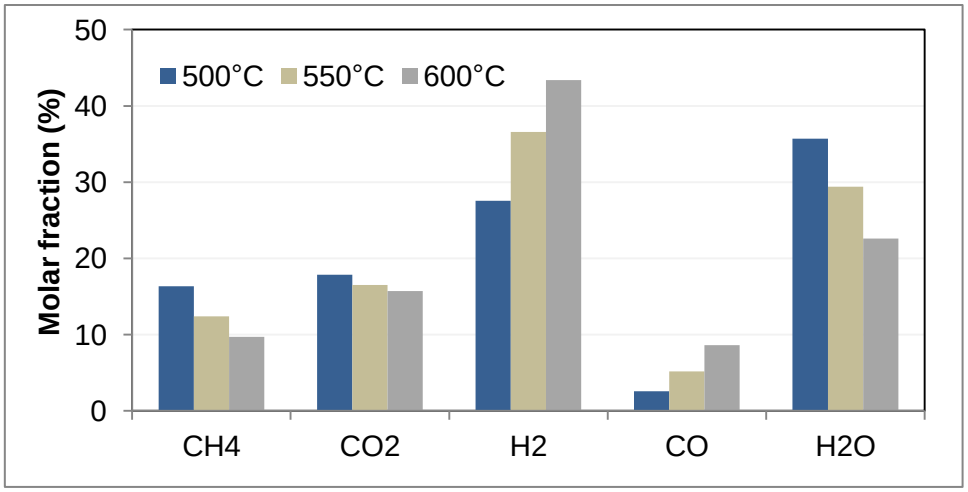

Figure 3.

Figure 4 in word format

Click here to download Figure(s): Figure 4 in word format.docx

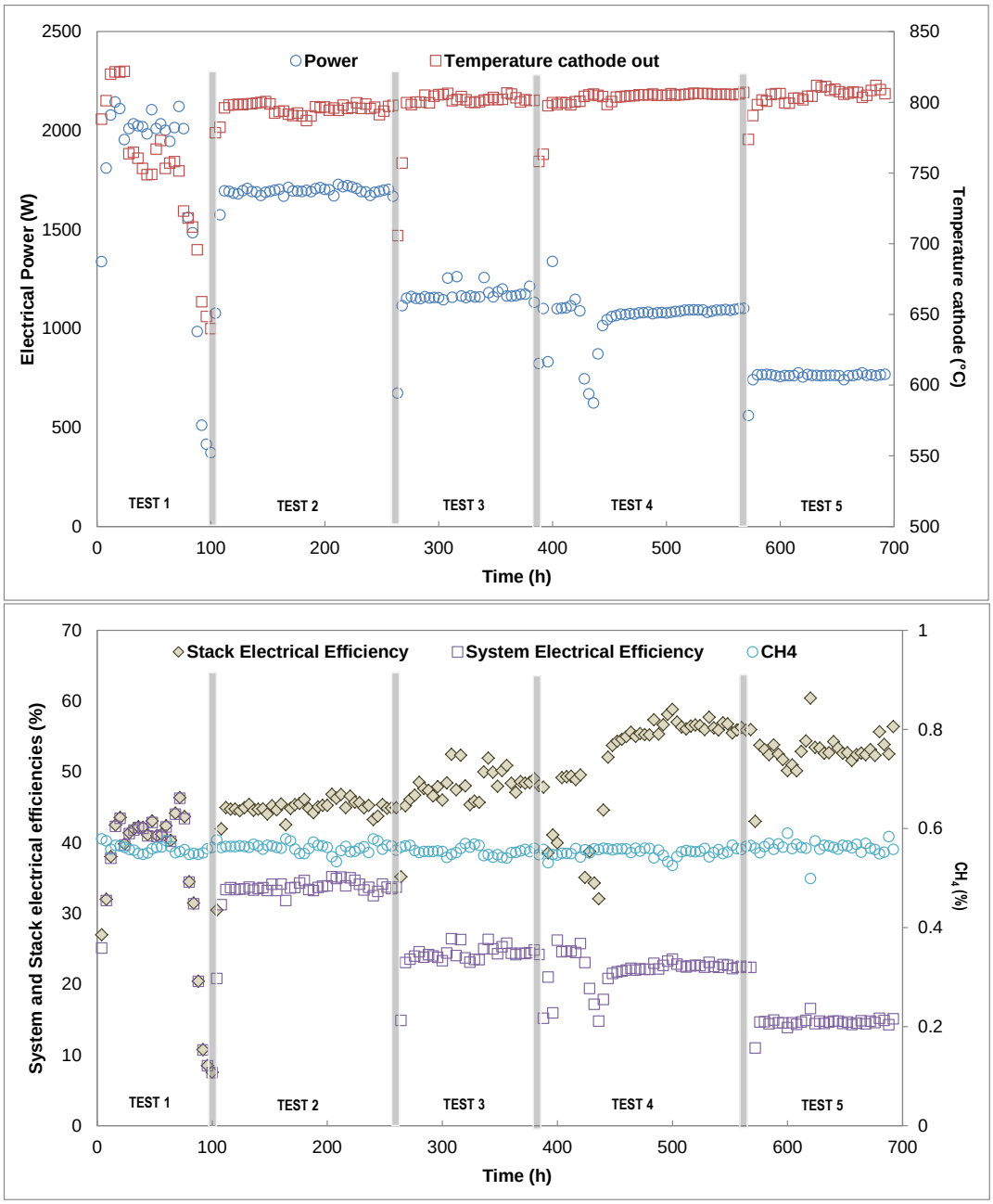

Figure 4.

Figure 5 in word format
Click here to download Figure(s): Figure 5 in word format.docx

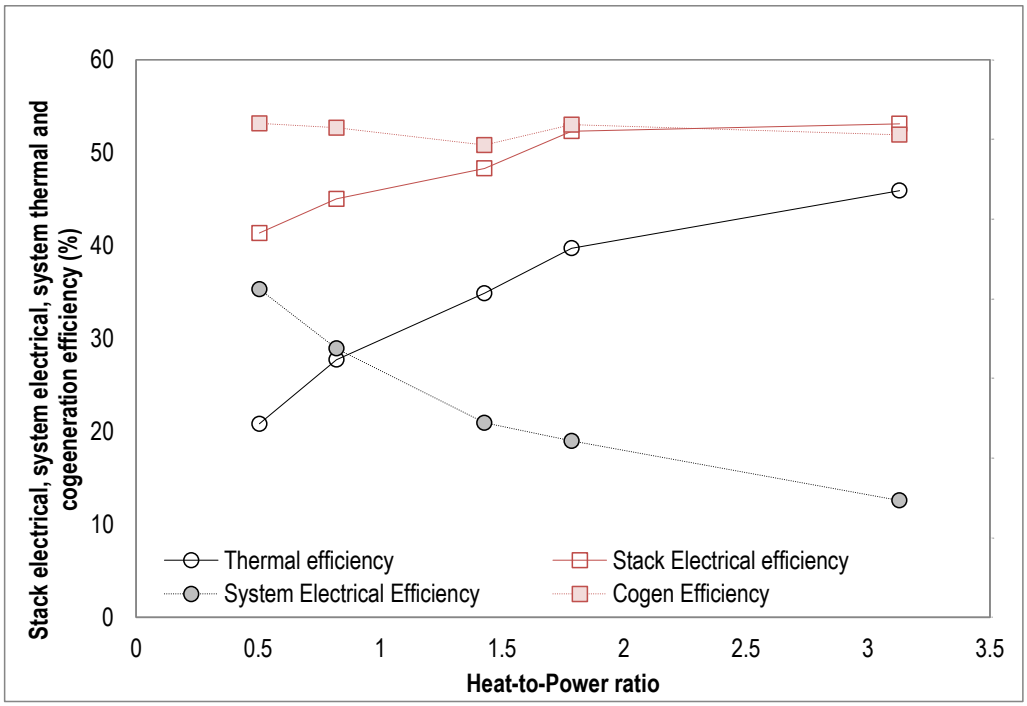

Figure 5.

Figure 6 in word format

Click here to download Figure(s): Figure 6 in word format.docx

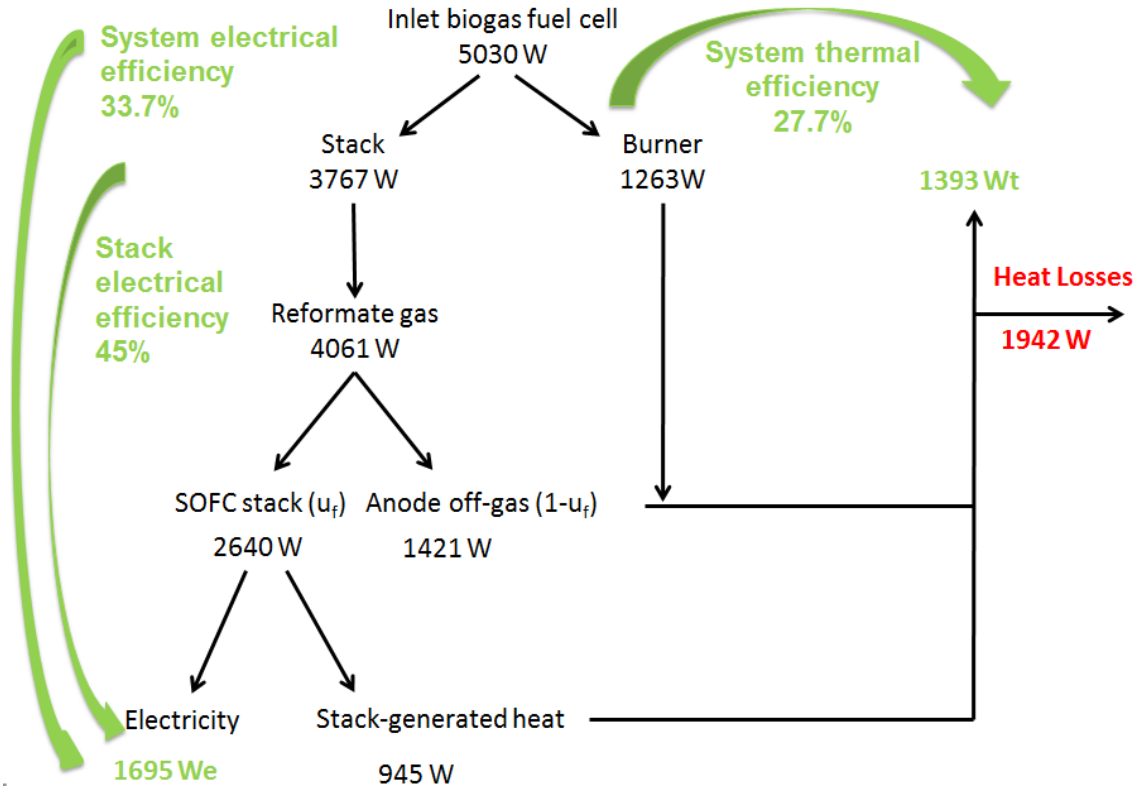

Figure 6.

Figure 7 in word format
Click here to download Figure(s): Figure 7 in word format.docx

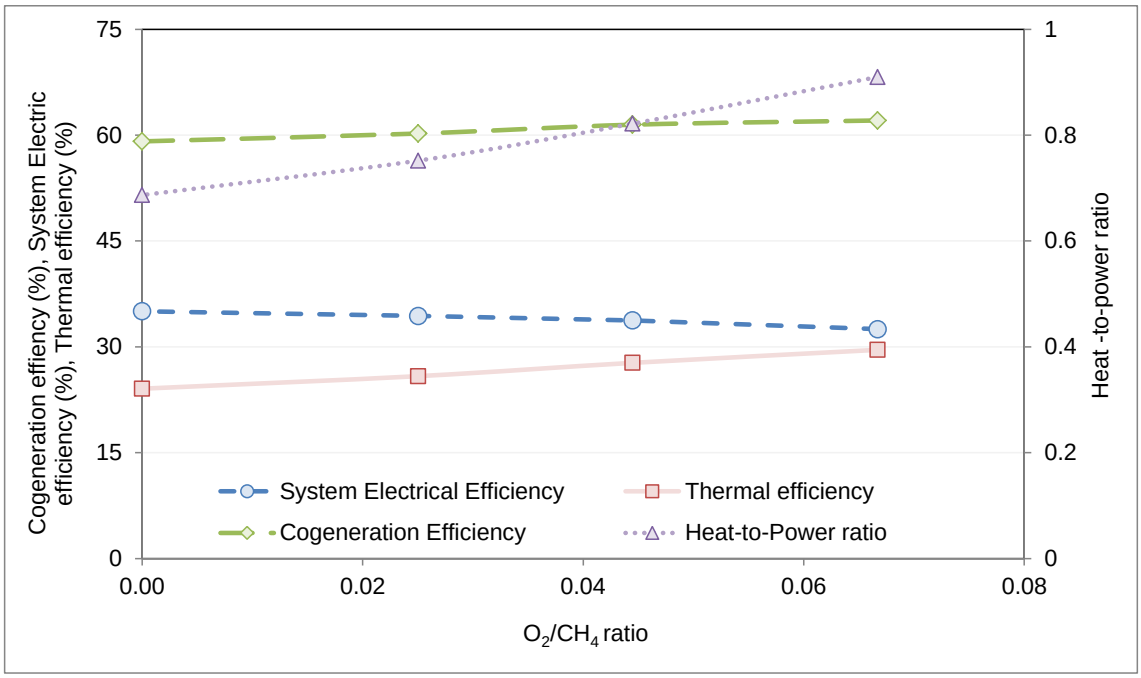

Figure 7.

Figure captions

Figure 1. Process Flow Diagram of the biogas-powered SOFC

Figure 2. Experimental test rig to evaluate soot formation limits

Figure 3. Molar composition of reformed biogas (CH_4:CO_2 60:40, O/C 2.1)

Figure 4. SOFC performance under different heat-to-power ratios: (a) electrical power and cathode outlet temperature; and (b) stack electrical efficiency, system electrical efficiency and methane content.

Figure 5. Effect of the heat-to-power ratio on the SOFC performance (electrical/thermal)

Figure 6. Energy balances biogas-powered SOFC at Test 2

Figure 7. Effect of the oxygen content in the biogas on the electrical, thermal and cogeneration efficiency; and the heat-to-power ratio